LMMSE-Aided WLLS Location Estimators for Source Localization with RSS Measurements

Donglin Zhang, Zhansheng Duan
Center for Information Engineering Science Research
Xi'an Jiaotong University
Xi'an, Shaanxi 710049, P.R. China
Email: zdlin23@stu.xjtu.edu.cn, zsduan@mail.xjtu.edu.cn

Yiyong Sun, Feng Yin
School of Science and Engineering
The Chinese University of Hong Kong
Shenzhen, Guangdong 518172, P.R. China
Email: yiyongsun@link.cuhk.edu.cn, yinfeng@cuhk.edu.cn

***Abstract*—Received signal strength (RSS) measurements can be converted to the distance estimates between the emission source and the sensors to construct a system of linear equations, thereby allowing for the use of the weighted linear least squares (WLLS) estimators for location estimation. However, estimating the squared distances from the RSS measurements governed by the log-normal shadowing effect presents a major challenge in such approaches. In this paper, we propose a linear minimum mean square error (LMMSE) estimator of the squared distance between the emission source and the sensor first. Then a LMMSE-aided WLLS (LMMSE-WLLS) location estimator and its unbiased counterpart are presented for source localization. Furthermore, their estimation performance are analyzed in terms of mean square error (MSE) and covariance. It is found that the proposed LMMSE-aided WLLS location estimators have better estimation performance than existing WLLS estimators. Numerical examples also demonstrate the performance superiority of the proposed location estimators for source localization.**

***Index Terms*—RSS, source localization, WLLS, LMMSE, wireless sensor networks.**

I. Introduction

Location estimation in wireless sensor networks (WSNs) is a fundamental and crucial issue due to the rapidly increasing demand for services that depend upon accurate positioning [1]. Many localization techniques have been developed [2–4]. They aim at estimating the locations of unknown sensors via noisy measurements [5]. In general, these measurements may include RSS, time of arrival (TOA), time difference of arrival (TDOA), and angle of arrival (AOA). Among them, TOA and TDOA require precise clock synchronization of sensors. AOA requires antenna arrays with radio-frequency front-end components [6]. These extra requirements result in complex implementation and higher power consumption. In contrast, the RSS measurement is a promising candidate mainly because of its low cost and complexity in hardware and software implementations.

In WSNs, multiple sensors are distributed with known locations, referred to as anchor nodes, and measure the strength of the signal emitted from the source whose location is unknown. Localization approaches are therefore employed to estimate the source location [7]. In general, the main approaches to tackle such source localization problems include proximity-based positioning, radio frequency (RF) fingerprinting, and distance-based positioning [8]. Among them, the distance-based approaches that use a log-distance path-loss propagation model are regarded as the mainstream, e.g., the maximum likelihood (ML) estimator [5], semidefinite programming (SDP) method [9, 10], and WLLS estimator [11–13].

In essence, source localization using RSS measurements is a nonlinear estimation problem. Therefore, the ML estimator is widely employed, usually serving as a performance benchmark for comparison with other location estimators. With ideal initialization, its estimation performance is very close to the Cramér–Rao lower bound (CRLB) [2, 9]. However, the optimization problem of the ML estimator is nonconvex and contains multiple local minima and maxima [10]. It is hard to implement in practice. Recently, application of convex relaxation techniques, e.g., SDP and second-order cone programming (SOCP), to source localization problem has received extensive attention [9, 14]. They relax the original nonconvex problem to a convex optimization problem, ensuring convergence to the global optimum [15]. However, non-simple mathematical form and high computational complexity are their main disadvantages.

Another typical approach to source localization is the WLLS estimator [13, 16]. Its basic idea is to estimate the distances between the emission source and the sensors from the RSS measurements, construct a system of linear equations, and then utilize the WLLS estimator to estimate the source location. Because of its closed-form solution, this approach is simple, computationally efficient, and widely applied in positioning applications [17]. As pointed out in [11, 12, 18], the estimation performance of the WLLS estimator is sensitive to the distance estimates between the emission source and the sensors. The approximate, biased, or suboptimal distance estimates will result in performance degradation. Many improved WLLS estimators have been proposed. In [19, 20], two WLLS estimators were proposed by using the ML estimate of the squared distance. With multiplicative debiasing strategy, a best linear unbiased estimator (BLUE) was presented in [21] and demonstrated in [22] that its performance is very close to that of the ML estimator using the Levenberg-Marquardt method. However, the estimation performance of these approaches is

This work is supported in part by National Key R&D Program of China under Grants 2021YFC2202600 and 2021YFC2202603.

much worse than the CRLB, particularly when the noise standard deviation is large. As a result, there is still potential to improve the estimation performance of the WLLS estimator. In this paper, we present two new WLLS location estimators for source localization, along with an analysis of their estimation performance.

The main contributions of this paper are twofold:

1) From the RSS measurement at each sensor, a LMMSE estimator of the squared distance between the emission source and the sensor is presented, thus leading to a LMMSE-WLLS location estimator for source localization. On this basis, a LMMSE-aided unbiased WLLS (LMMSE-UWLLS) location estimator is also presented.
2) Estimation performance of the proposed WLLS location estimators is analyzed in terms of MSE and covariance. The following is found. The LMMSE-WLLS location estimator performs better than the ML-WLLS estimator, and the LMMSE-UWLLS location estimator performs better than the BLUE estimator.

This paper is organized as follows. Section II formulates the problem of RSS source localization. Section III presents the proposed WLLS location estimators. Section IV analyzes their estimation performance. Illustrative examples are provided in Section V. Section VI concludes the paper.

II. Problem Formulation

Consider a WSN in a two-dimensional plane with n sensors (or anchor nodes) at known locations and one emission source at unknown location. Let $\boldsymbol{a}_i = [x_i, y_i]^T$, $i \in \mathbb{N} = \{1, 2, \cdots, n\}$, be the location of the i-th sensor, and $\boldsymbol{x}_s = [x, y]^T$ be the location of the emission source to be estimated. Then the RSS measurement P_i at the i-th sensor emitted from the source under the log-distance path-loss (or log-normal shadowing) model [4] is

$$P_i = P_0 - 10\alpha \log_{10}(d_i/d_0) + w_i \tag{1}$$

where

$$d_i = ||\boldsymbol{a}_i - \boldsymbol{x}_s||_2 \tag{2}$$

is the Euclidean distance between the emission source and the i-th sensor, P_0 is the reference power at a reference distance d_0, α is the path-loss exponent, typically related to the propagation environment, and w_i is zero-mean Gaussian measurement noise with variance σ_w^2, i.e., $w_i \sim \mathcal{N}(0, \sigma_w^2)$, assumed independent across sensors. Without loss of generality, it is also assumed that $d_0 = 1$m, and P_0 and α are known parameters [18–22].

For RSS source localization, RSS measurements can be converted to the distance estimates between the emission source and the sensors, leading to the source location $\boldsymbol{x}_s$ estimated by the WLLS estimator. To guarantee the estimability of this problem, at least two sensors are required [5]. Consider a central information processor that performs localization, with which all sensor nodes can communicate. Since a unique identifying tag is contained with each RSS measurement, data association is not needed here. In this paper, we aim to develop new WLLS location estimators for RSS source localization and analyze their estimation performance.

III. LMMSE-Aided WLLS Location Estimators

In this section, we present a LMMSE-WLLS location estimator for source localization. On this basis, an unbiased LMMSE-WLLS location estimator is also presented.

A. LMMSE-WLLS Location Estimator

From (1), the RSS measurement model can be rewritten as

$$d_i^2 = e^{\frac{-2r_i}{\alpha}} e^{\frac{2v_i}{\alpha}}, \ i \in \mathbb{N} \tag{3}$$

where

$$r_i = \frac{\ln 10}{10}(P_i - P_0) - \alpha \ln d_0 \tag{4}$$

$$v_i = \frac{\ln 10}{10} w_i \tag{5}$$

and v_i also follows Gaussian distribution $v_i \sim \mathcal{N}(0, \sigma_v^2)$ with $\sigma_v = (\ln 10/10)\sigma_w$.

It can be seen that the squared distance d_i^2 is a linear function of the term $e^{\frac{-2r_i}{\alpha}}$ with multiplicative noise term $e^{\frac{2v_i}{\alpha}}$. Let $z_i = e^{\frac{-2r_i}{\alpha}}$ being the pseudo measurement. Then we have

$$d_i^2 = z_i e^{\frac{2v_i}{\alpha}}, \ i \in \mathbb{N} \tag{6}$$

Note that the multiplicative noise term $e^{\frac{2v_i}{\alpha}}$ is not available in positioning applications but its statistics can be obtained from the RSS measurement noise statistics. Taking expectation of $e^{\frac{2v_i}{\alpha}}$ yields

$$E[e^{\frac{2v_i}{\alpha}}] = e^{\frac{2\sigma_v^2}{\alpha^2}} \tag{7}$$

Given pseudo measurement z_i, by utilizing the mean of (7), the squared distance d_i^2 can thus be estimated by

$$\widehat{d_i^2} = z_i e^{\frac{2\sigma_v^2}{\alpha^2}} \tag{8}$$

Similarly, the squared distance estimate in (8) is also a linear function of the pseudo measurement z_i, accompanied by the multiplicative factor $e^{\frac{2\sigma_v^2}{\alpha^2}}$. We are interested in whether alternative squared distance estimates can be obtained with other different multiplicative factors. Toward this end, define a general multiplicative factor η. Then a unified form of the squared distance estimate can be obtained as

$$\widehat{d_i^2} = \eta z_i \tag{9}$$

and its corresponding MSE is[1]

$$\begin{aligned}\text{MSE}(\widehat{d_i^2}) &= d_i^4 \eta^2 e^{\frac{4\sigma_v^2}{\alpha^2}} (e^{\frac{4\sigma_v^2}{\alpha^2}} - 1) + d_i^4 (\eta e^{\frac{2\sigma_v^2}{\alpha^2}} - 1)^2 \\ &= d_i^4 [\eta^2 e^{\frac{8\sigma_v^2}{\alpha^2}} - 2\eta e^{\frac{2\sigma_v^2}{\alpha^2}} + 1]\end{aligned} \tag{10}$$

Minimizing the MSE of (10) with respect to η yields

$$\eta^{\text{LMMSE}} = \arg\min_{\eta} \ d_i^4 [\eta^2 e^{\frac{8\sigma_v^2}{\alpha^2}} - 2\eta e^{\frac{2\sigma_v^2}{\alpha^2}} + 1] = e^{\frac{-6\sigma_v^2}{\alpha^2}} \tag{11}$$

[1]For scalar variable d, if $\widehat{d}$ represents its estimate, then the MSE of $\widehat{d}$ is denoted as $\text{MSE}(\widehat{d}) \triangleq E[(d - \widehat{d})^2]$, and its estimation error variance is denoted as $\text{var}(\widehat{d}) \triangleq E[(\widetilde{d} - E[\widetilde{d}])^2]$.

Substituting (11) into (9), the LMMSE estimate of the squared distance can then be obtained as

$$\widehat{d_i^2}^{\text{LMMSE}} = z_i e^{-\frac{6\sigma_v^2}{\alpha^2}} \tag{12}$$

Let

$$\widetilde{d_i^2} = d_i^2 - \widehat{d_i^2} \tag{13}$$

be the estimation error of $\widehat{d_i^2}$. Then the expectation and variance of estimation error of the LMMSE estimate $\widehat{d_i^2}^{\text{LMMSE}}$ are[1]

$$E[\widetilde{d_i^2}^{\text{LMMSE}}] = d_i^2(1 - e^{\frac{-4\sigma_v^2}{\alpha^2}}) \tag{14}$$

$$\text{var}(\widetilde{d_i^2}^{\text{LMMSE}}) = d_i^4 e^{\frac{-8\sigma_v^2}{\alpha^2}}(e^{\frac{4\sigma_v^2}{\alpha^2}} - 1) \tag{15}$$

and the MSE of $\widehat{d_i^2}^{\text{LMMSE}}$ is

$$\text{MSE}(\widehat{d_i^2}^{\text{LMMSE}}) = d_i^4 e^{\frac{-8\sigma_v^2}{\alpha^2}}(e^{\frac{4\sigma_v^2}{\alpha^2}} - 1) + d_i^4(e^{\frac{-4\sigma_v^2}{\alpha^2}} - 1)^2 \tag{16}$$

Next, we estimate the source location $\boldsymbol{x}_s$ by utilizing the obtained squared distance estimates between the emission source and the sensors. From (2) and (13), given the squared distance estimate of each sensor, a system of nonlinear equations can be constructed as

$$\begin{aligned}\widehat{d_i^2} &= \| \boldsymbol{a}_i - \boldsymbol{x}_s \|_2^2 - \widetilde{d_i^2} \\ &= -2x_i x - 2y_i y + \vartheta + \kappa_i - \widetilde{d_i^2}\end{aligned} \tag{17}$$

where $\vartheta = x^2 + y^2$ and $\kappa_i = x_i^2 + y_i^2,\ i \in \mathbb{N}$.

To convert (17) into a system of linear equations, two schemes are generally employed. One is to define a new quantity ϑ to be estimated. The other is to subtract a reference equation from the remaining equations of (17), thereby eliminating the quantity ϑ. Selecting the l-th equation of (17) as the reference equation, we have[2]

$$\begin{aligned}\widehat{d_{i'}^2} - \widehat{d_l^2} = &-2(x_{i'} - x_l)x - 2(y_{i'} - y_l)y \\ &+ \kappa_{i'} - \kappa_l - \widetilde{d_{i'}^2} + \widetilde{d_l^2}\end{aligned} \tag{18}$$

where $i' \in \mathbb{N}\backslash l$, and $\mathbb{N}\backslash l$ represents set difference, that is, $\mathbb{N}\backslash l$ is set $\mathbb{N}$ without element l.

As a result, the compact matrix form of (18) is

$$\boldsymbol{y} = \boldsymbol{G}\boldsymbol{x}_s + \boldsymbol{v} \tag{19}$$

where

$$\boldsymbol{y} = \begin{bmatrix} \widehat{d_{1'}^2} - \widehat{d_l^2} - \kappa_{1'} + \kappa_l \\ \vdots \\ \widehat{d_{m'}^2} - \widehat{d_l^2} - \kappa_{m'} + \kappa_l \end{bmatrix}, \boldsymbol{v} = \begin{bmatrix} \widetilde{d_l^2} - \widetilde{d_{1'}^2} \\ \vdots \\ \widetilde{d_l^2} - \widetilde{d_{m'}^2} \end{bmatrix}$$

$$\boldsymbol{G} = -2\begin{bmatrix} x_{1'} - x_l & y_{1'} - y_l \\ \vdots & \vdots \\ x_{m'} - x_l & y_{m'} - y_l \end{bmatrix}$$

[2]The symbol i' represents one of the elements in $\mathbb{N}\backslash l$, $i = 1, \cdots, m$, and $m = n - 1$. For example, for set $\mathbb{N} = \{1, 2, 3, 4, 5\}$, $n = 5$, if $l = 3$, then $\mathbb{N}\backslash l = \{1, 2, 4, 5\}$, and a one-to-one correspondence between i', $i' \in \{1, 2, 4, 5\}$ and i, $i = 1, 2, 3, 4$ is that $1' = 1$, $2' = 2$, $3' = 4$, and $4' = 5$.

and the covariance of $\boldsymbol{v}$ is

$$\boldsymbol{R} \triangleq \text{cov}(\boldsymbol{v}) = \begin{bmatrix} \text{var}(\widetilde{d_{1'}^2}) + \text{var}(\widetilde{d_l^2}) & \text{var}(\widetilde{d_l^2}) & \cdots & \text{var}(\widetilde{d_l^2}) \\ \text{var}(\widetilde{d_l^2}) & \text{var}(\widetilde{d_{2'}^2}) + \text{var}(\widetilde{d_l^2}) & \cdots & \text{var}(\widetilde{d_l^2}) \\ \vdots & \vdots & \ddots & \vdots \\ \text{var}(\widetilde{d_l^2}) & \text{var}(\widetilde{d_l^2}) & \cdots & \text{var}(\widetilde{d_{m'}^2}) + \text{var}(\widetilde{d_l^2}) \end{bmatrix} \tag{20}$$

Using the inverse of $\boldsymbol{R}$ as weighting matrix, the WLLS location estimator is therefore obtained by minimizing the following cost function

$$\boldsymbol{J}(\boldsymbol{x}_s) = (\boldsymbol{y} - \boldsymbol{G}\boldsymbol{x}_s)^T \boldsymbol{R}^{-1}(\boldsymbol{y} - \boldsymbol{G}\boldsymbol{x}_s)$$

and is given by

$$\hat{\boldsymbol{x}}_s^{\text{WLLS}} = (\boldsymbol{G}^T\boldsymbol{R}^{-1}\boldsymbol{G})^{-1}\boldsymbol{G}^T\boldsymbol{R}^{-1}\boldsymbol{y} \tag{21}$$

Substituting the LMMSE estimate of the squared distance of (12) into (21), then the LMMSE-aided WLLS (LMMSE-WLLS) location estimator can be obtained as

$$\begin{aligned}\hat{\boldsymbol{x}}_s^{\text{LMMSE-WLLS}} =& (\boldsymbol{G}^T(\boldsymbol{R}^{\text{LMMSE}})^{-1}\boldsymbol{G})^{-1}\boldsymbol{G}^T \\ &\times (\boldsymbol{R}^{\text{LMMSE}})^{-1}\boldsymbol{y}^{\text{LMMSE}}\end{aligned} \tag{22}$$

where

$$\boldsymbol{y}^{\text{LMMSE}} = \begin{bmatrix} e^{-\frac{2r_{1'}}{\alpha} - \frac{6\sigma_v^2}{\alpha^2}} - e^{-\frac{2r_l}{\alpha} - \frac{6\sigma_v^2}{\alpha^2}} - \kappa_{1'} + \kappa_l \\ \vdots \\ e^{-\frac{2r_{m'}}{\alpha} - \frac{6\sigma_v^2}{\alpha^2}} - e^{-\frac{2r_l}{\alpha} - \frac{6\sigma_v^2}{\alpha^2}} - \kappa_{m'} + \kappa_l \end{bmatrix} \tag{23}$$

and

$$\begin{aligned}\boldsymbol{R}^{\text{LMMSE}} =& \text{diag}(d_{1'}^4 e^{\frac{-8\sigma_v^2}{\alpha^2}}(e^{\frac{4\sigma_v^2}{\alpha^2}} - 1), \cdots, d_{m'}^4 e^{\frac{-8\sigma_v^2}{\alpha^2}}(e^{\frac{4\sigma_v^2}{\alpha^2}} - 1) \\ &+ d_l^4 e^{\frac{-8\sigma_v^2}{\alpha^2}}(e^{\frac{4\sigma_v^2}{\alpha^2}} - 1)\mathbf{1}_m\end{aligned} \tag{24}$$

$\mathbf{1}_m$ represents an m-dimensional matrix with all elements being 1.

Since d_i^2, $i \in \mathbb{N}$, is unavailable in positioning applications, $\boldsymbol{R}^{\text{LMMSE}}$ can be approximated by replacing d_i^2 in (24) with its LMMSE estimate, given by

$$\begin{aligned}\widehat{\boldsymbol{R}}^{\text{LMMSE}} =& \text{diag}(e^{\frac{-4r_{1'} - 20\sigma_v^2}{\alpha}}(e^{\frac{4\sigma_v^2}{\alpha^2}} - 1), \cdots, e^{\frac{-4r_{m'} - 20\sigma_v^2}{\alpha}} \\ &\times (e^{\frac{4\sigma_v^2}{\alpha^2}} - 1) + e^{\frac{-4r_l - 20\sigma_v^2}{\alpha}}(e^{\frac{4\sigma_v^2}{\alpha^2}} - 1)\mathbf{1}_m\end{aligned} \tag{25}$$

In addition, it is possible to set the weighting matrix $\boldsymbol{R}^{\text{LMMSE}}$ in (22) to an identity matrix, leading to the following corresponding LMMSE-LLS location estimator

$$\hat{\boldsymbol{x}}_s^{\text{LMMSE-LLS}} = (\boldsymbol{G}^T\boldsymbol{G})^{-1}\boldsymbol{G}^T\boldsymbol{y}^{\text{LMMSE}} \tag{26}$$

Remark 1: The estimation performance of the WLLS estimator does not depend on the selection of reference equation [5], due to the use of the optimal weighting matrix, i.e., the inverse of $\boldsymbol{R}$. Thus, the reference equation index l in (21) can be selected arbitrarily from the set $\mathbb{N}$, e.g., $l = 1$ or 3.

B. LMMSE-UWLLS Location Estimator

Similarly to (21), the unbiased WLLS (UWLLS) location estimator can be obtained as

$$\hat{\boldsymbol{x}}_s^{\text{UWLLS}} = (\boldsymbol{G}^T\boldsymbol{R}^{-1}\boldsymbol{G})^{-1}\boldsymbol{G}^T\boldsymbol{R}^{-1}\boldsymbol{y}^{\text{u}} \tag{27}$$

where

$$\begin{aligned}\boldsymbol{y}^{\text{u}} &= \boldsymbol{y} - E[\boldsymbol{v}]\\ &= \begin{bmatrix}\widehat{d_{1'}^2} - \widehat{d_l^2} - \kappa_{1'} + \kappa_l\\ \vdots\\ \widehat{d_{m'}^2} - \widehat{d_l^2} - \kappa_{m'} + \kappa_l\end{bmatrix} - \begin{bmatrix}E[\widetilde{d_l^2}] - E[\widetilde{d_{1'}^2}]\\ \vdots\\ E[\widetilde{d_l^2}] - E[\widetilde{d_{m'}^2}]\end{bmatrix}\end{aligned} \tag{28}$$

and the weighting matrix $\boldsymbol{R}$ is the same as in the WLLS estimator (21) and is given by (20).

Then the LMMSE-UWLLS location estimator can be obtained as

$$\begin{aligned}\hat{\boldsymbol{x}}_s^{\text{LMMSE-UWLLS}} =&(\boldsymbol{G}^T(\boldsymbol{R}^{\text{LMMSE}})^{-1}\boldsymbol{G})^{-1}\boldsymbol{G}^T\\ &\times(\boldsymbol{R}^{\text{LMMSE}})^{-1}\boldsymbol{y}^{\text{LMMSE-u}}\end{aligned} \tag{29}$$

where $\boldsymbol{y}^{\text{LMMSE-u}}$ is obtained by substituting the squared distance estimate of (12) and its estimation error expectation of (14) into (28), and the weighting matrix $\boldsymbol{R}^{\text{LMMSE}}$ is given by (24). Since d_i^2, $i \in \mathbb{N}$, is unknown, approximated form in (25) can be employed in practice. In addition, the expectation of estimation error in (28) can also be approximated by replacing d_i^2 with its estimate in (12).

IV. Performance Analysis

In this section, estimation performance of the proposed location estimators is analyzed by comparison with the existing WLLS estimators.

As in [19, 20], the ML estimate of the squared distance is

$$\widehat{d_i^2}^{\text{ML}} = \arg\max_{d_i^2} L(d_i^2|P_i) = d_0^2 e^{\frac{\ln 10}{5\alpha}(P_0 - P_i)} = e^{\frac{-2r_i}{\alpha}} \tag{30}$$

where

$$L(d_i^2|P_i) = \frac{1}{\sqrt{2\pi}\sigma_w}e^{-\frac{1}{2\sigma_w^2}(P_i - P_0 + 5\alpha\log_{10}(d_i^2/d_0^2))^2} \tag{31}$$

is the likelihood function of d_i^2 given by model (1). Then the ML-WLLS location estimator [19, 20] can be obtained as

$$\hat{\boldsymbol{x}}_s^{\text{ML-WLLS}} = (\boldsymbol{G}^T(\boldsymbol{R}^{\text{ML}})^{-1}\boldsymbol{G})^{-1}\boldsymbol{G}^T(\boldsymbol{R}^{\text{ML}})^{-1}\boldsymbol{y}^{\text{ML}} \tag{32}$$

where

$$\boldsymbol{y}^{\text{ML}} = \begin{bmatrix}e^{\frac{-2r_{1'}}{\alpha}} - e^{\frac{-2r_l}{\alpha}} - \kappa_{1'} + \kappa_l\\ \vdots\\ e^{\frac{-2r_{m'}}{\alpha}} - e^{\frac{-2r_l}{\alpha}} - \kappa_{m'} + \kappa_l\end{bmatrix} \tag{33}$$

is obtained by substituting the ML estimate in (30) into (21), and

$$\begin{aligned}\boldsymbol{R}^{\text{ML}} =&\text{diag}(d_{1'}^4 e^{\frac{4\sigma_v^2}{\alpha^2}}(e^{\frac{4\sigma_v^2}{\alpha^2}} - 1), \cdots, d_{m'}^4 e^{\frac{4\sigma_v^2}{\alpha^2}}(e^{\frac{4\sigma_v^2}{\alpha^2}} - 1)\\ &+ d_l^4 e^{\frac{4\sigma_v^2}{\alpha^2}}(e^{\frac{4\sigma_v^2}{\alpha^2}} - 1)\boldsymbol{1}_m\end{aligned} \tag{34}$$

Similarly, with multiplicative debiasing, the ML-UWLLS (or BLUE-WLLS) location estimator in [21, 22] can be obtained as

$$\hat{\boldsymbol{x}}_s^{\text{BLUE-WLLS}} = (\boldsymbol{G}^T(\boldsymbol{R}^{\text{BLUE}})^{-1}\boldsymbol{G})^{-1}\boldsymbol{G}^T(\boldsymbol{R}^{\text{BLUE}})^{-1}\boldsymbol{y}^{\text{BLUE}} \tag{35}$$

where

$$\boldsymbol{y}^{\text{BLUE}} = \begin{bmatrix}e^{\frac{-2r_{1'}}{\alpha} - \frac{2\sigma_v^2}{\alpha^2}} - e^{\frac{-2r_l}{\alpha} - \frac{2\sigma_v^2}{\alpha^2}} - \kappa_{1'} + \kappa_l\\ \vdots\\ e^{\frac{-2r_{m'}}{\alpha} - \frac{2\sigma_v^2}{\alpha^2}} - e^{\frac{-2r_l}{\alpha} - \frac{2\sigma_v^2}{\alpha^2}} - \kappa_{m'} + \kappa_l\end{bmatrix} \tag{36}$$

and

$$\begin{aligned}\boldsymbol{R}^{\text{BLUE}} =&\text{diag}(d_{1'}^4(e^{\frac{4\sigma_v^2}{\alpha^2}} - 1), \cdots, d_{m'}^4(e^{\frac{4\sigma_v^2}{\alpha^2}} - 1)\\ &+ d_l^4(e^{\frac{4\sigma_v^2}{\alpha^2}} - 1)\boldsymbol{1}_m\end{aligned} \tag{37}$$

Remark 2: Note that the ML-WLLS and BLUE-WLLS location estimators can also be obtained by substituting $\eta = 1$ and $\eta = e^{\frac{-2\sigma_v^2}{\alpha^2}}$ into (21), respectively. Therefore, they belong to the unified form (21) of the WLLS estimator. In addition, we have proposed three pseudo conditional distributed induced WLLS estimators in [18]. These location estimators can also be obtained from (21) using other multiplicative factors.

Let $\boldsymbol{P} = [-\boldsymbol{1}_{m\times1}, \boldsymbol{I}_m]$, and

$$\boldsymbol{y}_0 = \begin{bmatrix}d_{1'}^2 - d_l^2 - \kappa_{1'} + \kappa_l\\ \vdots\\ d_{m'}^2 - d_l^2 - \kappa_{m'} + \kappa_l\end{bmatrix}, \quad \boldsymbol{y}_0^l = \begin{bmatrix}d_l^2 - \kappa_l\\ d_{1'}^2 - \kappa_{1'}\\ \vdots\\ d_{m'}^2 - \kappa_{m'}\end{bmatrix} \tag{38}$$

where $\boldsymbol{1}_{m\times1}$ represents an m-dimensional column vector with all elements being 1. Since $\boldsymbol{G}$ is of full column rank, the source location $\boldsymbol{x}_s$ can be represented as

$$\boldsymbol{x}_s = \boldsymbol{V}^\dagger\boldsymbol{y}_0 = \boldsymbol{V}^\dagger\boldsymbol{P}\boldsymbol{y}_0^l \tag{39}$$

where

$$\boldsymbol{V}^\dagger = (\boldsymbol{G}^T\boldsymbol{R}_0\boldsymbol{G})^{-1}\boldsymbol{G}^T(\boldsymbol{R}_0)^{-1} \tag{40}$$

and $\boldsymbol{R}_0 = \boldsymbol{P}\ \text{diag}(d_l^4, d_{1'}^4, \cdots, d_{m'}^4)\boldsymbol{P}^T$.

Let $\xi = e^{\frac{-8\sigma_v^2}{\alpha^2}}(e^{\frac{4\sigma_v^2}{\alpha^2}} - 1)$. Then we have

$$\begin{aligned}\boldsymbol{V}^\dagger &= (\boldsymbol{G}^T(\xi\boldsymbol{R}_0)^{-1}\boldsymbol{G})^{-1}\boldsymbol{G}^T(\xi\boldsymbol{R}_0)^{-1}\\ &= (\boldsymbol{G}^T(\boldsymbol{R}^{\text{LMMSE}})^{-1}\boldsymbol{G})^{-1}\boldsymbol{G}^T(\boldsymbol{R}^{\text{LMMSE}})^{-1}\end{aligned} \tag{41}$$

For the ML-WLLS and BLUE-WLLS estimators, similar $\boldsymbol{V}^\dagger$ can be obtained by simply replacing $\boldsymbol{R}^{\text{LMMSE}}$ with $\boldsymbol{R}^{\text{ML}}$ and $\boldsymbol{R}^{\text{BLUE}}$, respectively. Similarly, the WLLS estimator of (21) can be rewritten as

$$\hat{\boldsymbol{x}}_s^{\text{WLLS}} = \boldsymbol{V}^\dagger\boldsymbol{y} = \boldsymbol{V}^\dagger\boldsymbol{P}\boldsymbol{y}^l \tag{42}$$

where $\boldsymbol{y}^l = [\widehat{d_l^2} - \kappa_l, \widehat{d_{1'}^2} - \kappa_{1'}, \cdots, \widehat{d_{m'}^2} - \kappa_{m'}]^T$, $i' \in \mathbb{N}\backslash l$.

Then the MSE of the WLLS estimator $\hat{\boldsymbol{x}}_s^{\text{WLLS}}$ is

$$\begin{aligned}\text{MSE}(\hat{\boldsymbol{x}}_s^{\text{WLLS}}) &= E[(\boldsymbol{x}_s - \hat{\boldsymbol{x}}_s^{\text{WLLS}})(\boldsymbol{x}_s - \hat{\boldsymbol{x}}_s^{\text{WLLS}})^T]\\ &= \boldsymbol{V}^\dagger\boldsymbol{P}E[(\boldsymbol{y}_0^l - \boldsymbol{y}^l)(\boldsymbol{y}_0^l - \boldsymbol{y}^l)^T](\boldsymbol{V}^\dagger\boldsymbol{P})^T\\ &= \boldsymbol{V}^\dagger\boldsymbol{P}\text{MSE}(\widehat{\boldsymbol{d}_l^2})(\boldsymbol{V}^\dagger\boldsymbol{P})^T\end{aligned} \tag{43}$$

where $\widehat{\boldsymbol{d}_l^2} = [\widehat{d_l^2}, \widehat{d_{1'}^2}, \cdots, \widehat{d_{m'}^2}]^T$, $i' \in \mathbb{N}\backslash l$,

$$\text{MSE}(\widehat{\boldsymbol{d}_l^2}) = \begin{bmatrix} \text{MSE}(\widehat{d_l^2}) & E[\widetilde{d_l^2}]E[\widetilde{d_{1'}^2}] & \cdots & E[\widetilde{d_l^2}]E[\widetilde{d_{m'}^2}] \\ E[\widetilde{d_{1'}^2}]E[\widetilde{d_l^2}] & \text{MSE}(\widehat{d_{1'}^2}) & \cdots & E[\widetilde{d_{1'}^2}]E[\widetilde{d_{m'}^2}] \\ \vdots & \vdots & \ddots & \vdots \\ E[\widetilde{d_{m'}^2}]E[\widetilde{d_l^2}] & E[\widetilde{d_{m'}^2}]E[\widetilde{d_{1'}^2}] & \cdots & \text{MSE}(\widehat{d_{m'}^2}) \end{bmatrix} \quad (44)$$

and all elements of $\text{MSE}(\widehat{\boldsymbol{d}_l^2})$ are given by (14) and (16).

The covariance of $\hat{\boldsymbol{x}}_s^{\text{WLLS}}$ is

$$\begin{aligned} \text{cov}(\hat{\boldsymbol{x}}_s^{\text{WLLS}}) &= E[(\hat{\boldsymbol{x}}_s^{\text{WLLS}} - E[\hat{\boldsymbol{x}}_s^{\text{WLLS}}])(\hat{\boldsymbol{x}}_s^{\text{WLLS}} - E[\hat{\boldsymbol{x}}_s^{\text{WLLS}}])^T] \\ &= \boldsymbol{V}^\dagger E[(\boldsymbol{y} - E[\boldsymbol{y}])(\boldsymbol{y} - E[\boldsymbol{y}])^T](\boldsymbol{V}^\dagger)^T \\ &= \boldsymbol{V}^\dagger \boldsymbol{R} (\boldsymbol{V}^\dagger)^T \end{aligned} \quad (45)$$

where

$$\begin{aligned} \boldsymbol{R} &= \boldsymbol{P}\text{cov}(\widetilde{\boldsymbol{d}_l^2})\boldsymbol{P}^T \\ &= \boldsymbol{P}\text{diag}(\text{var}(\widetilde{d_l^2}), \text{var}(\widetilde{d_{1'}^2}), \cdots, \text{var}(\widetilde{d_{m'}^2}))\boldsymbol{P}^T \end{aligned} \quad (46)$$

and $\widetilde{\boldsymbol{d}_l^2} = [d_l^2, d_{1'}^2, \cdots, d_{m'}^2]^T - \widehat{\boldsymbol{d}_l^2}$, $i' \in \mathbb{N}\backslash l$.

Next, we discuss estimation performance of the proposed LMMSE-WLLS location estimator in terms of the MSE and covariance. Compared to the existing ML-WLLS location estimator, the following theorem holds.

Theorem 1: In terms of MSE and covariance, the LMMSE-WLLS and ML-WLLS location estimators satisfy

$$\text{MSE}(\hat{\boldsymbol{x}}_s^{\text{LMMSE-WLLS}}) \leq \text{MSE}(\hat{\boldsymbol{x}}_s^{\text{ML-WLLS}}) \quad (47)$$
$$\text{cov}(\hat{\boldsymbol{x}}_s^{\text{LMMSE-WLLS}}) \leq \text{cov}(\hat{\boldsymbol{x}}_s^{\text{ML-WLLS}}) \quad (48)$$

where all equalities hold if and only if $\sigma_w = 0$.

Proof: see Appendix A.

As can be seen from Theorem 1, the proposed LMMSE-WLLS location estimator outperforms the existing ML-WLLS estimator in terms of both MSE and covariance. Note that if identity matrix instead of the inverse of $\boldsymbol{R}$ is used as the weighting matrix, Theorem 1 still holds.

For the UWLLS estimator, the MSE of $\hat{\boldsymbol{x}}_s^{\text{UWLLS}}$ can be obtained as

$$\begin{aligned} \text{MSE}(\hat{\boldsymbol{x}}_s^{\text{UWLLS}}) &= E[(\boldsymbol{x}_s - \hat{\boldsymbol{x}}_s^{\text{UWLLS}})(\boldsymbol{x}_s - \hat{\boldsymbol{x}}_s^{\text{UWLLS}})^T] \\ &= \boldsymbol{V}^\dagger E[(\boldsymbol{y}_0 - \boldsymbol{y}^{\text{u}})(\boldsymbol{y}_0 - \boldsymbol{y}^{\text{u}})^T](\boldsymbol{V}^\dagger)^T \\ &= \boldsymbol{V}^\dagger E[(\boldsymbol{y} - E[\boldsymbol{y}])(\boldsymbol{y} - E[\boldsymbol{y}])^T](\boldsymbol{V}^\dagger)^T \\ &= \boldsymbol{V}^\dagger \boldsymbol{R} (\boldsymbol{V}^\dagger)^T \end{aligned} \quad (49)$$

and its covariance is identical to the MSE. Note that $\boldsymbol{R}$ is given by (46).

Compared to the BLUE-WLLS location estimator, we have the following theorem.

Theorem 2: In terms of MSE and covariance, the LMMSE-UWLLS and BLUE-WLLS location estimators satisfy

$$\text{MSE}(\hat{\boldsymbol{x}}_s^{\text{LMMSE-UWLLS}}) \leq \text{MSE}(\hat{\boldsymbol{x}}_s^{\text{BLUE-WLLS}}) \quad (50)$$
$$\text{cov}(\hat{\boldsymbol{x}}_s^{\text{LMMSE-UWLLS}}) \leq \text{cov}(\hat{\boldsymbol{x}}_s^{\text{BLUE-WLLS}}) \quad (51)$$

where all equalities hold if and only if $\sigma_w = 0$.

Proof: see Appendix B.

For these two unbiased location estimators, the proposed LMMSE-UWLLS estimator has better estimation performance than the BLUE-WLLS estimator. Therefore, it is recommended in positioning applications.

TABLE I: Compared location estimators.

Name	Description
η_1-WLLS	WLLS estimator (21) using $\eta = e^{\frac{3\sigma_v^2}{\alpha^2}}$.
η_2-WLLS	WLLS estimator (21) using $\eta = e^{\frac{2\sigma_v^2}{\alpha^2}}$.
ML-WLLS	Maximum-likelihood WLLS estimator [19, 20].
BLUE-WLLS	Best linear unbiased estimator [21, 22].
SOCP	Second-order cone programming [14].
SDP-l_1	Semidefinite programming using l_1 norm [10].
SDP-l_2	Semidefinite programming using l_2 norm [9].
CWLS	Constrained weighted least squares estimator [10].
ML-truth	Maximum likelihood estimator initialized with the true source location [5].
LMMSE-WLLS	LMMSE-WLLS estimator in (22).
LMMSE-UWLLS	LMMSE-UWLLS estimator in (29).

V. Illustrative Examples

In this section, numerical examples are provided to evaluate estimation performance of the proposed location estimators, as well as demonstrating their effectiveness. All compared algorithms are listed in Table I. Note that the η_1-WLLS and η_2-WLLS location estimators are obtained by substituting $\eta = e^{\frac{3\sigma_v^2}{\alpha^2}}$ and $\eta = e^{\frac{2\sigma_v^2}{\alpha^2}}$ into (21), respectively. The SOCP, SDP-l_1, SDP-l_2, and CWLS estimators are implemented by the CVX toolbox using SeDuMi [23]. The ML estimator is implemented numerically with the MATLAB routine $\mathrm{lsqnonlin}$ using the Levenberg–Marquardt method with ideal initialization. In addition, the Cramér-Rao lower bound (CRLB) [2] is also considered for comparison purpose.

As in [9, 14, 18], two experimental scenarios are considered, differing in the deployments of the emission source and sensors. In the first scenario (S1), eight sensors are evenly deployed in a 20m $\times$ 20m square area, and the emission source to be estimated is located in the square area inside the convex hull of the sensors. Fig. 1(a) shows the deployment of the emission source and sensors for S1. In the second scenario (S2), as shown in Fig. 1(b), the same number of sensors are deployed irregularly in the square area, but the emission source is located outside the convex hull of the sensors.

Without loss of generality, the path-loss exponent is set to $\alpha = 4$, and the reference power is set to $P_0 = -50$dBm, as in [9, 10, 18, 21]. The standard deviation σ_w of measurement noise varies from 1 to 5dB [4]. All results bellow are averaged over 500 Monte Carlo runs.

A. Effect of Noise Standard Deviation

First, we evaluate estimation performance of the proposed location estimators versus the noise standard deviation. The performance evaluation metric adopted is root mean squared

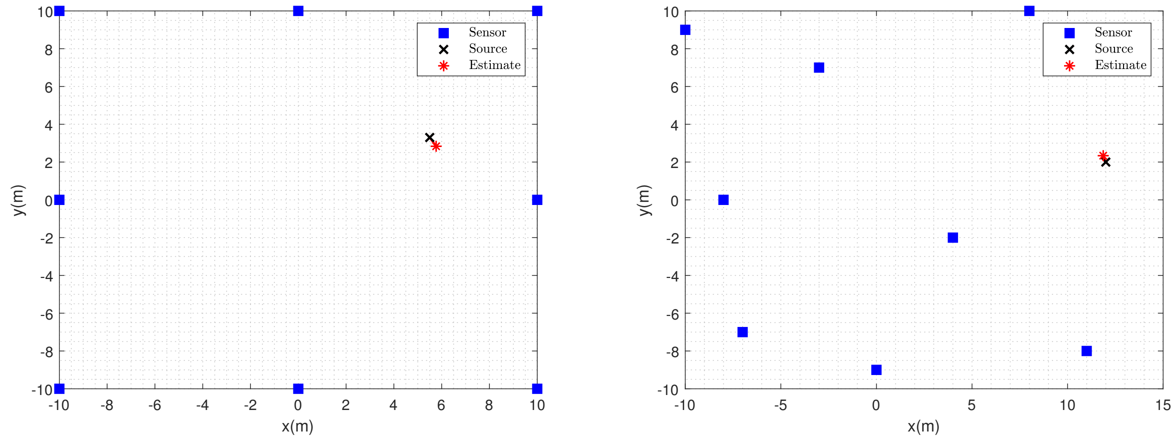

(a) S1 (b) S2

Fig. 1: Two scenarios of deployments of emission source and sensors. The blue solid squares represent the sensors, the black cross represents the emission source, and the red asterisk represents the location estimate of the emission source.

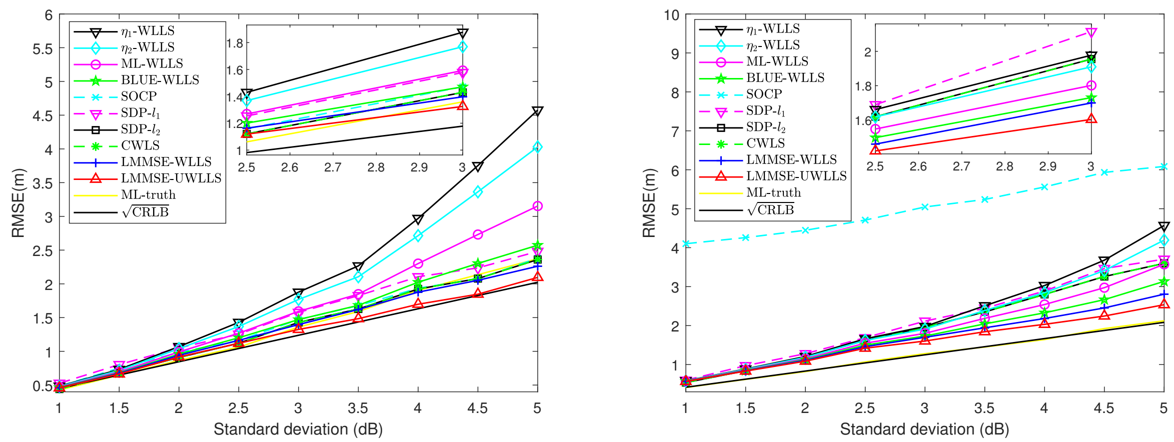

(a) S1 (b) S2

Fig. 2: RMSEs of compared location estimators versus noise standard deviation.

error (RMSE). As the noise standard deviation increases, the RMSE increases gradually. Fig. 2(a) shows the RMSEs of the compared location estimators for S1. It can be seen that the proposed LMMSE-WLLS and LMMSE-UWLLS location estimators always outperform the η_1-WLLS, η_2-WLLS, ML-WLLS, and BLUE-WLLS estimators significantly, especially when the noise standard deviation is large. Compared to the convex optimization algorithms including SOCP, SDP-l_1, SDP-l_2, and CWLS, our proposed LMMSE-WLLS location estimator has better estimation performance for most noise standard deviations. The LMMSE-UWLLS location estimator has the best estimation performance for all noise standard deviations, and its performance is very close to that of the ML-truth estimator and the CRLB. These results demonstrate the effectiveness of the proposed location estimators as well.

Fig. 2(b) shows the RMSEs of the compared location estimators for S2. It can be seen that the proposed LMMSE-WLLS and LMMSE-UWLLS location estimators perform better the existing WLLS estimators significantly. When the emission source is located outside the convex hull of the sensors, both the LMMSE-WLLS and LMMSE-UWLLS location estimators outperform the SDP-l_1, SDP-l_2, and CWLS estimators for all noise standard deviations. This demonstrates their effectiveness again. Note that the SOCP method cannot be applied in this case because its estimate always lies within the convex hull of the sensors [14, 18].

B. Effect of Number of Sensors

Second, we evaluate estimation performance of the proposed location estimators versus the number of sensors. As shown in Fig. 3, the proposed LMMSE-WLLS and LMMSE-UWLLS location estimators have better performance than the existing WLLS estimators for both S1 and S2. When the number of sensors is large, the RMSE of the LMMSE-UWLLS estimator

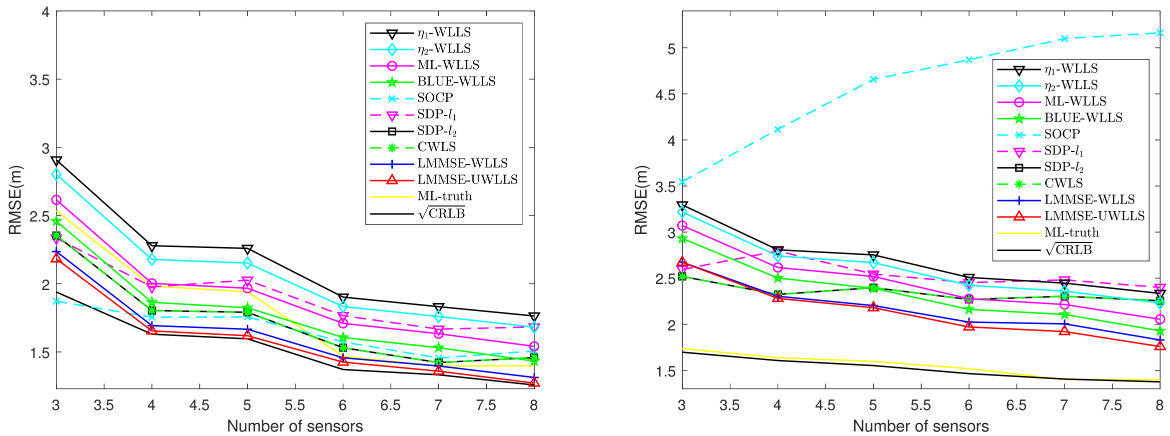

(a) S1 (b) S2

Fig. 3: RMSEs of compared location estimators versus number of sensors.

is very close to the square root of the CRLB. Compared to the convex optimization algorithms, the proposed location estimators always outperform the SOCP and SDP-l_1 estimators, and also outperform the SDP-l_2 and CWLS estimators for most sensor numbers. This also demonstrates the effectiveness of the proposed location estimators. As the number of sensors increases, the constraints of the SOCP problem become tighter. Therefore, the RMSE of the SOCP estimator in S2 increases gradually.

VI. Conclusions

In this paper, we have investigated the source localization problem using RSS measurements. Two new WLLS location estimators have been proposed, utilizing the LMMSE estimates of the squared distances between the emission source and the sensors from the RSS measurements. In addition, estimation performance of the LMMSE-aided WLLS location estimators has been analyzed by comparison with other existing WLLS estimators for source localization. It is found that in terms of MSE and covariance, the LMMSE-WLLS location estimator performs better than the ML-WLLS estimator, and the LMMSE-UWLLS location estimator performs better than the BLUE-WLLS estimator. Numerical experiments have also verified these, and shown that the proposed two WLLS location estimators outperform the convex optimization algorithms compared in most cases. Future work will investigate the source localization problem when the path-lose exponent and reference power are not known exactly.

Appendix A
Proof of Theorem 1

For the MSEs of the LMMSE-WLLS and ML-WLLS location estimators, let

$$\boldsymbol{M} = \text{MSE}(\hat{\boldsymbol{x}}_s^{\text{ML-WLLS}}) - \text{MSE}(\hat{\boldsymbol{x}}_s^{\text{LMMSE-WLLS}}) \tag{52}$$

Then it follows that

$$\boldsymbol{M} = \boldsymbol{V}^{\dagger}\boldsymbol{P}\boldsymbol{D}(\boldsymbol{V}^{\dagger}\boldsymbol{P})^T \tag{53}$$

where

$$\boldsymbol{D} = \text{MSE}(\widehat{\boldsymbol{d}_l^2}^{\text{ML}}) - \text{MSE}(\widehat{\boldsymbol{d}_l^2}^{\text{LMMSE}}) \tag{54}$$

Both $\text{MSE}(\widehat{\boldsymbol{d}_l^2}^{\text{LMMSE}})$ and $\text{MSE}(\widehat{\boldsymbol{d}_l^2}^{\text{ML}})$ are positive semi-definite, and they are zero if and only if $\sigma_w = 0$.

Substituting (12) and (30) into (54), then $\boldsymbol{D}$ is given by[3]

$$\begin{aligned} [\boldsymbol{D}]_{ii} &= \text{MSE}(\widehat{d_{r'}^2}^{\text{ML}}) - \text{MSE}(\widehat{d_{r'}^2}^{\text{LMMSE}}) \\ &= d_{r'}^4(e^{\frac{4\sigma_v^2}{\alpha^2}} - e^{\frac{-8\sigma_v^2}{\alpha^2}})(e^{\frac{4\sigma_v^2}{\alpha^2}} - 1) + d_{r'}^4((e^{\frac{2\sigma_v^2}{\alpha^2}} \\ &\quad - 1)^2 - (e^{\frac{-4\sigma_v^2}{\alpha^2}} - 1)^2) \end{aligned} \tag{55}$$

$$\begin{aligned} [\boldsymbol{D}]_{ij} &= E[\widetilde{d_{r'}^2}^{\text{ML}}\widetilde{d_{k'}^2}^{\text{ML}}] - E[\widetilde{d_{r'}^2}^{\text{LMMSE}}\widetilde{d_{k'}^2}^{\text{LMMSE}}] \\ &= d_{r'}^2 d_{k'}^2((e^{\frac{2\sigma_v^2}{\alpha^2}} - 1)^2 - (e^{\frac{-4\sigma_v^2}{\alpha^2}} - 1)^2) \end{aligned} \tag{56}$$

where $i, j = 1, \cdots, n$, $i \neq j$, $r = i-1$, $k = j-1$, $0' = l$, and all elements of $\boldsymbol{D}$ are positive, i.e., $[\boldsymbol{D}]_{ii} > 0, [\boldsymbol{D}]_{ij} > 0$.

Let

$$\zeta = (e^{\frac{4\sigma_v^2}{\alpha^2}} - e^{\frac{-8\sigma_v^2}{\alpha^2}})(e^{\frac{4\sigma_v^2}{\alpha^2}} - 1) \tag{57}$$

$$\gamma = (e^{\frac{2\sigma_v^2}{\alpha^2}} - 1)^2 - (e^{\frac{-4\sigma_v^2}{\alpha^2}} - 1)^2 \tag{58}$$

Then we have

$$[\boldsymbol{D}]_{ii} = d_{(i-1)'}^4(\zeta + \gamma),\ [\boldsymbol{D}]_{ij} = d_{(i-1)'}^2 d_{(j-1)'}^2\gamma \tag{59}$$

Next, $\boldsymbol{D}$ is proved to be positive definite. That is, all principal minors of $\boldsymbol{D}$ are positive[4].

The 1-th principal minor of $\boldsymbol{D}$ is

$$|\boldsymbol{D}|_{1\times 1} = d_l^4(\zeta + \gamma) > 0$$

The 2-th principal minor of $\boldsymbol{D}$ is

$$|\boldsymbol{D}|_{2\times 2} = d_l^4 d_{1'}^4[\zeta^2 + 2\zeta\gamma] > 0 \tag{60}$$

[3]Note that $[\boldsymbol{D}]_{ij}$ stands for the i-th row and j-th column element of $\boldsymbol{D}$.
[4]The i-th principal minor of $\boldsymbol{D}$ is denoted as $|\boldsymbol{D}|_{i\times i}$, $i \in \mathbb{N}$.

Assume that the i-th principal minor of $\boldsymbol{D}$ satisfies

$$|\boldsymbol{D}|_{i\times i} = d_l^4 d_{1'}^4 \cdots d_{(i-1)'}^4 [(\zeta+\gamma)^i + (i-1)\gamma^i - i(\zeta+b)\gamma^{i-1}] = d_l^4 \cdots d_{(i-1)'}^4 [\zeta^i + C_i^1 \zeta^{i-1}\gamma + \cdots + C_i^{i-2}\zeta^2\gamma^{i-2}] > 0 \tag{61}$$

Then the $(i+1)$-th principal minor of $\boldsymbol{D}$ is

$$|\boldsymbol{D}|_{(i+1)\times(i+1)} = d_l^4 d_{1'}^4 \cdots d_{i'}^4 [(\zeta+\gamma)^{i+1} + i\gamma^{i+1} - (i+1)(\zeta+\gamma)\gamma^i] \tag{62}$$

Since $|\boldsymbol{D}|_{i\times i} > 0$, we have

$$\begin{aligned} &|\boldsymbol{D}|_{(i+1)\times(i+1)} \\ &= d_l^4 d_{1'}^4 \cdots d_{i'}^4 [\zeta^{i+1} + C_{i+1}^1 \zeta^i \gamma + \cdots + C_{i+1}^{i-1}\zeta^2\gamma^{i-1}] \\ &= d_l^4 d_{1'}^4 \cdots d_{i'}^4 \left[\frac{|\boldsymbol{D}|_{i\times i}}{d_l^4 \cdots d_{(i-1)'}^4}(\zeta+\gamma) + i\zeta^2\gamma^{i-1} \right] > 0 \end{aligned}$$

Thus all principal minors of $\boldsymbol{D}$ are positive and $\boldsymbol{D}$ is positive definite.

There exists a nonzero vector $\boldsymbol{x}$ such that $\boldsymbol{x}^T = \boldsymbol{y}^T \boldsymbol{V}^\dagger \boldsymbol{P}$ and $\boldsymbol{x}^T \boldsymbol{D} \boldsymbol{x} > 0$. Then we have

$$\boldsymbol{y}^T \boldsymbol{M} \boldsymbol{y} = \boldsymbol{y}^T \boldsymbol{V}^\dagger \boldsymbol{P} \boldsymbol{D} (\boldsymbol{V}^\dagger \boldsymbol{P})^T \boldsymbol{y} = \boldsymbol{x}^T \boldsymbol{D} \boldsymbol{x} > 0 \tag{63}$$

Thus $\boldsymbol{M}$ is also positive definite. From (52), we have

$$\mathrm{MSE}(\hat{\boldsymbol{x}}_s^{\text{LMMSE-WLLS}}) \leq \mathrm{MSE}(\hat{\boldsymbol{x}}_s^{\text{ML-WLLS}}) \tag{64}$$

where the equality holds if and only if $\sigma_w = 0$.

For the covariances of the LMMSE-WLLS and ML-WLLS location estimators, we have

$$\mathrm{var}(\widetilde{d_i^2}^{\text{LMMSE}}) \leq \mathrm{var}(\widetilde{d_i^2}^{\text{ML}}) \tag{65}$$

Then from (46), the covariance matrices satisfy

$$\boldsymbol{R}^{\text{LMMSE}} \leq \boldsymbol{R}^{\text{ML}} \tag{66}$$

Hence we have

$$\mathrm{cov}(\hat{\boldsymbol{x}}_s^{\text{LMMSE-WLLS}}) \leq \mathrm{cov}(\hat{\boldsymbol{x}}_s^{\text{ML-WLLS}}) \tag{67}$$

This completes the proof of Theorem 1.

Appendix B
Proof of Theorem 2

The MSE of the UWLLS location estimators is

$$\mathrm{MSE}(\hat{\boldsymbol{x}}_s^{\text{UWLLS}}) = \boldsymbol{V}^\dagger \boldsymbol{R} (\boldsymbol{V}^\dagger)^T \tag{68}$$

From the proof of Theorem 1, we have

$$\boldsymbol{R}^{\text{LMMSE}} \leq \boldsymbol{R}^{\text{ML}} \tag{69}$$

Therefore, the MSEs of the LMMSE-UWLLS and BLUE-WLLS location estimators satisfy

$$\mathrm{MSE}(\hat{\boldsymbol{x}}_s^{\text{LMMSE-UWLLS}}) \leq \mathrm{MSE}(\hat{\boldsymbol{x}}_s^{\text{BLUE-WLLS}}) \tag{70}$$

It is known that the covariance and MSE of the unbiased estimator are identical [5]. As a result, we also have

$$\mathrm{cov}(\hat{\boldsymbol{x}}_s^{\text{LMMSE-UWLLS}}) \leq \mathrm{cov}(\hat{\boldsymbol{x}}_s^{\text{BLUE-WLLS}}) \tag{71}$$

This completes the proof of Theorem 2.

References

[1] F. Zafari, A. Gkelias, and K. K. Leung, "A survey of indoor localization systems and technologies," *IEEE Communications Surveys and Tutorials*, vol. 21, no. 3, pp. 2568–2599, 2019.

[2] N. Patwari, J. N. Ash, S. Kyperountas, A. O. Hero, R. L. Moses, and N. S. Correal, "Locating the nodes: cooperative localization in wireless sensor networks," *IEEE Signal Processing Magazine*, vol. 22, no. 4, pp. 54–69, 2005.

[3] J. He, Y. J. Chun, and H. C. So, "A unified analytical framework for RSS-based localization systems," *IEEE Internet of Things Journal*, vol. 9, no. 9, pp. 6506–6519, 2022.

[4] T. S. Rappaport, *Wireless Communications : Principles and Practice*. Upper Saddle River: NJ: Prentice-Hall, 2002.

[5] S. A. Zekavat and R. M. Buehrer, *Handbook of Position Location: Theory, Practice, and Advances*. New York: John Wiley & Sons, 2019.

[6] S. Xu and K. Dogancay, "Optimal sensor placement for 3-D angle-of-arrival target localization," *IEEE Transactions on Aerospace and Electronic Systems*, vol. 53, no. 3, pp. 1196–1211, 2017.

[7] R. M. Buehrer, H. Wymeersch, and R. M. Vaghefi, "Collaborative sensor network localization: Algorithms and practical issues," *Proceedings of the IEEE*, vol. 106, no. 6, pp. 1089–1114, 2018.

[8] G. M. Bianco, R. Giuliano, F. Mazzenga, and G. Marrocco, "Multi-slope path loss and position estimation with grid search and experimental results," *IEEE Transactions on Signal and Information Processing over Networks*, vol. 7, pp. 551–561, 2021.

[9] R. M. Vaghefi, M. R. Gholami, R. M. Buehrer, and E. G. Strom, "Cooperative received signal strength-based sensor localization with unknown transmit powers," *IEEE Transactions on Signal Processing*, vol. 61, no. 6, pp. 1389–1403, 2013.

[10] Q. Wang, Z. S. Duan, and X. R. Li, "Three-dimensional location estimation using biased RSS measurements," *IEEE Transactions on Aerospace and Electronic Systems*, vol. 56, no. 6, pp. 4673–4688, 2020.

[11] S. D. Chitte, S. Dasgupta, and Z. Ding, "Distance estimation from received signal strength under log-normal shadowing: Bias and variance," *IEEE Signal Processing Letters*, vol. 16, no. 3, pp. 216–218, 2009.

[12] S. Mazuelas, A. Bahillo, R. M. Lorenzo, P. Fernandez, F. A. Lago, E. Garcia, J. Blas, and E. J. Abril, "Robust indoor positioning provided by real-time RSSI values in unmodified WLAN networks," *IEEE Journal of Selected Topics in Signal Processing*, vol. 3, no. 5, pp. 821–831, 2009.

[13] S. Wu, D. Xu, and S. Liu, "Weighted linear least square localization algorithms for received signal strength," *Wireless personal communications*, vol. 72, no. 1, pp. 747–757, 2013.

[14] S. Tomic, M. Beko, and R. Dinis, "RSS-based localization in wireless sensor networks using convex relaxation: Noncooperative and cooperative schemes," *IEEE Transactions on Vehicular Technology*, vol. 64, no. 5, pp. 2037–2050, 2015.

[15] S. Salari, S. Shahbazpanahi, and K. Ozdemir, "Mobility-aided wireless sensor network localization via semidefinite programming," *IEEE Transactions on Wireless Communications*, vol. 12, no. 12, pp. 5966–5978, 2013.

[16] L. X. Lin, H. C. So, and Y. T. Chan, "Received signal strength based positioning for multiple nodes in wireless sensor networks," *Digital Signal Processing*, vol. 25, pp. 41–50, 2014.

[17] H. Ketabalian, M. Biguesh, and A. Sheikhi, "A closed-form solution for localization based on RSS," *IEEE Transactions on Aerospace and Electronic Systems*, vol. 56, no. 2, pp. 912–923, 2020.

[18] D. L. Zhang and Z. S. Duan, "Pseudo conditional distribution induced radio source localisation using received signal strength measurements," *IET Radar, Sonar & Navigation*, vol. 17, no. 12, pp. 1768–1784, 2023.

[19] N. Salman, A. H. Kemp, and M. Ghogho, "Low complexity joint estimation of location and path-loss exponent," *IEEE Wireless Communications Letters*, vol. 1, no. 4, pp. 364–367, 2012.

[20] P. Tarrio, A. M. Bernardos, J. A. Besada, and J. R. Casar, "A new positioning technique for RSS-based localization based on a weighted least squares estimator," in *Proceedings of 2008 IEEE International Symposium on Wireless Communication Systems*, Oct 2008.

[21] H. C. So and L. X. Lin, "Linear least squares approach for accurate received signal strength based source localization," *IEEE Transactions on Signal Processing*, vol. 59, no. 8, pp. 4035–4040, Aug 2011.

[22] L. X. Lin and H. C. So, "Best linear unbiased estimator algorithm for received signal strength based localization," in *Proceedings of 2011 European Signal Processing Conference*, Barcelona, Spain, Aug 2011.

[23] J. F. Sturm, *Using SeDuMi 1.02, a MATLAB Toolbox for Optimization Over Symmetric Cones*. Upper Saddle River: Prentice Hall PTR, 1998.